Energy-Saving in Air Conditioners Using PLC Control and the SCADA Monitoring System

Waluyo†, **Andre Widura**, and **Wahyu Agung Purbandoko**, Non-members

ABSTRACT

The promotion of energy-saving air conditioners (ACs) continues to increase. Therefore, this research proposes the implementation of automatic control and monitoring for AC fan evaporator and compressor speeds using a programmable logic controller (PLC) along with supervisory control and data acquisition (SCADA). The proposed system uses a room-temperature sensor, connected to the PLC and programmed with a ladder diagram. It is connected to a SCADA installed computer for monitoring and data logging. The testing involves three methods: conventional, manual, and automatic PLC-based. Over a four-week period, the conventional method consumed 193.6 kW·h, 198.7 kW·h, and 206.6 kW·h in energy, while the manual method consumed 160.5 kW·h, 160.1 kW·h, and 161.9 kW·h, and the automatic method 150.8 kW·h, 152.6 kW·h, and 154.8 kW·h using the trapezoidal composite rule, Simpson's composite rule, and ordinary methods, respectively. The main research contribution is the provision of an energy-saving system for air conditioners over a long duration using PLC. The PLC-based automatic-to-manual energy savings equate to 6.0%, 5.8%, and 4.4%; whereas 22.0%, 24.0%, and 25.0% for the PLC-based automatic-to-conventional method. Therefore, the PLC-based automatic control is deemed appropriate for electrical energy-saving.

Keywords: Air Conditioner, Energy-Saving, Programmable Logic Controller, PLC, Simpson's Composite, Trapezoidal Composite

1. INTRODUCTION

An air conditioner (AC) is a machine designed to stabilize the air temperature in a room at a certain time. Generally, it uses a refrigeration cycle but occasionally evaporative cooling is employed for its convenience in buildings and motor vehicles. Specifically, an AC unit cools the air by circulating refrigerant gas in a pipe, which is compressed by a compressor. The heat in the condenser pipe comes from the refrigerant gas so that the air becomes hot in the automatic expansion valve, where the refrigerant gas circulation is decreased, the pressure increases, and the evaporator pipe cools [1–3]. The standard procedure for the technical planning of energy conservation in buildings divides the comfortable temperature into three categories: cool (20.5–22.8 ℃), optimal (22.8–25.8 ℃), and warm (25.8–27.1 ℃) [4].

Many efforts have been made for energy-saving on air conditioners, usually involving hardware, such as a control valve to regulate the chilled water flow rate [5]. A new specialized program and a combination of supply and demand sides were found to improve energy efficiency [6–7]. For an automobile AC, energy-saving by waste-heat driven adsorption in the heat recovery system has been found to reduce the cooling power by 4% [8]. An energy-saving rate of 33% has been obtained by a rule-based fuzzy control method (RBFCM) [9], while a network platform involving a fan coil unit (FCU) and fuzzy control also produced energy savings [10]. A local-event-based method for heating, ventilation, and air conditioning (HVAC) control can achieve a near-optimal solution [11]. The learning-based token scheduling algorithm (LBTSA) on HVAC was found to provide enhanced energy savings of 5.6% with a token-based scheduling strategy (TBSS) [12]. Smart ACs have the potential to reduce energy costs [13].

A PLC is an industrial standard electronic device and can be used in air conditioning systems [14]. However, PLC-based energy-saving AC systems are limited and tend to involve fuzzy [15] or proportional-integral-derivative (PID) control [5, 16]. Used with a variable speed drive, the PLC provides greater AC efficiency [17] since its solenoid valve periodically opens and closes [18] the electronic expansion valve by regulating the steps [19] for solar direct expansion (DX) hybrid-air conditioning energy-saving [20], to control the various regeneration temperatures [21], data acquisition [22–23], on/off air conditioning [24], act as a master smart control terminal [10], as well as adjusting, processing, and regenerating air [25].

Based on the above studies, it is necessary to conduct further research on energy-saving for air conditioning using PLC, as an industrial standard over a long duration, for evaporator, compressor, and condenser controlling systems. This research employed a 4–20 mA analog input for temperature and humidity sensing signal transmission, with SCADA software for monitoring and data logging, and was found to consume less energy compared to conventional or manual operation. The energy consumed was computed using three methods for

Manuscript received on June 14, 2021; revised on August 10, 2021; accepted on September 7, 2021. This paper was recommended by Associate Editor Matheepot Phattanasak.

The authors are with the Department of Electrical Engineering, Institut Teknologi Nasional Bandung (ITENAS), Indonesia.

†Corresponding author: waluyo@itenas.ac.id

Digital Object Identifier: 10.37936/ecti-eec.2022201.246095

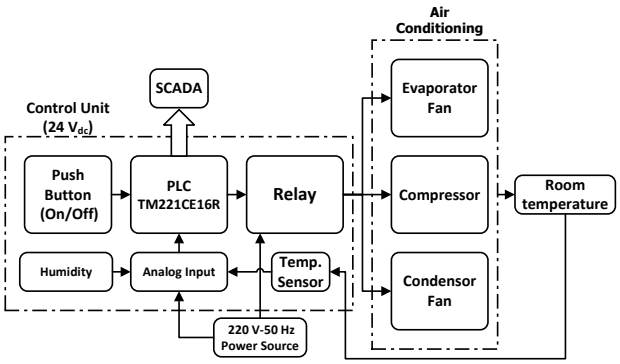

Fig. 1: *PLC-based air conditioning energy-saving diagram.*

Table 1: *Equipment specifications.*

Components	Specification
Portable AC	9000 Btu (1 set) 12000 Btu (2 sets)
PLC	9 input, 7 output
Input analog module	4–20 mA, 0–10 V
Temperature sensor	−19.9–60.0 °C, 4–20 mA
Humidity sensor	0.0–99.9%, 4–20 mA
Current instrument	0–5 A, 4–20 mA
Relay	24 Vdc coil, 220 V contact
Current Transformer	30 A/5 A

fair comparison, while the trending data analysis used box plot median values for robustness. These are new ideas and contribute to the existing research.

2. RESEARCH METHOD

The research design was tested on operational air conditioners in a laboratory restroom, controlled automatically by PLC and monitored and data logged remotely by SCADA. The PLC received information from the temperature sensor through the transmission of a 4–20 mA analog signal. The temperatures were set in the PLC program to determine the operation of the automatic control of the AC according to comfortable room conditions. The system was divided into two parts: software and hardware. The PLC and SCADA used SoMachine Basic v1.4 and Vijeo Citect, software, respectively. This program was designed to set the on/off switch to provide an automatic AC operation according to comfort requirements and display the temperature, relative humidity (RH), and consumed power, locally and remotely, as shown in Fig. 1. Temperature and humidity sensors detect the room conditions and send the data to the analog input module on the PLC. Likewise, the power consumed by the air conditioner is also presented in Fig. 1.

The PLC output digital signals were connected to a 24 Vdc relay coil, and the contacts to the 220 Vac source to run the compressor, condenser, and evaporator fans. The evaporator fan has three modes: high, medium, and low. Therefore, three compressors and three modes need

(a)

(b)

Fig. 2: *Installation of the portable ACs; (a) proposed design and (b) real condition.*

to be controlled by the PLC. The loading current was measured along with the running system, and the data sent to the PLC analog input module of 4–20 mA. The data were also sent to the SCADA installed computer for monitoring and recording, via wireless and the local area network (LAN). The size of the conditioned room was 3.5 m (11.48 ft), 4 m (13.12 ft), and 3 m (9.84 ft) in width, length, and height, respectively. The room was on the 4^{th} floor (top floor), and the longest south-facing wall. Thus, the AC capacity approached 9000 Btu. The total capacity of the portable ACs was two sets with 12000 Btu each and one set of 9000 Btu. The specifications of the main equipment used are listed in Table 1. The installation design of the three AC units in the room is shown in Fig. 2(a). The portable ACs were installed in parallel near the windows because they require heat dissipation to the outside room. Two ACs were installed in the corners of the room to reach the temperature in those positions, whereas the remaining AC was installed in the middle position as the primary temperature conditioner. The real installation of the three portable AC units is shown in Fig. 2(b).

The control system was programmed and downloaded

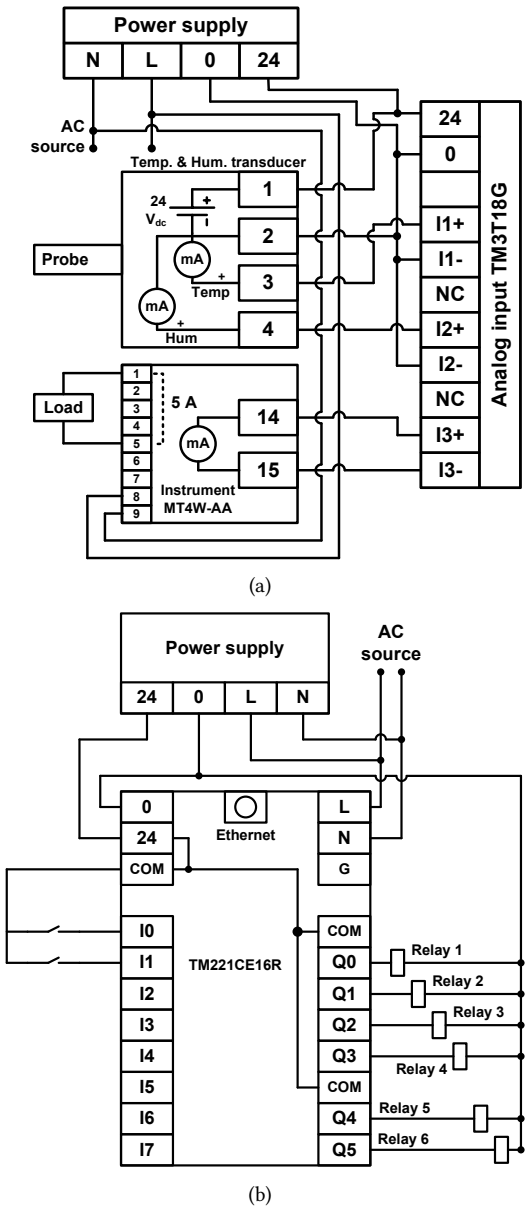

Fig. 3: *(a) Analog input and (b) digital output wiring diagrams.*

into the PLC input and output. The sensors measured the temperature, humidity, and current, transmitting the signals to the analog input of the PLC. Therefore, the PLC required additional equipment for the analog input module. The PLC was M221 type, TM221CE16R series, supplied by 220 V, 50 Hz. Whereas the analog input was TM3AI8/G series, supplied by 24 Vdc. The current was measured using a 5 A maximum reading sensor. The temperature and humidity sensor was installed in the center of the room where people were active. The wiring diagram of the analog input is shown in Fig. 3(a). The current measuring instrument then read the loading alternating current and sent it to the analog input of 4–20 mA. The PLC had a digital output, and the coils operated on 24 Vdc, as shown in Fig. 3(b). The relay distributed the power supply

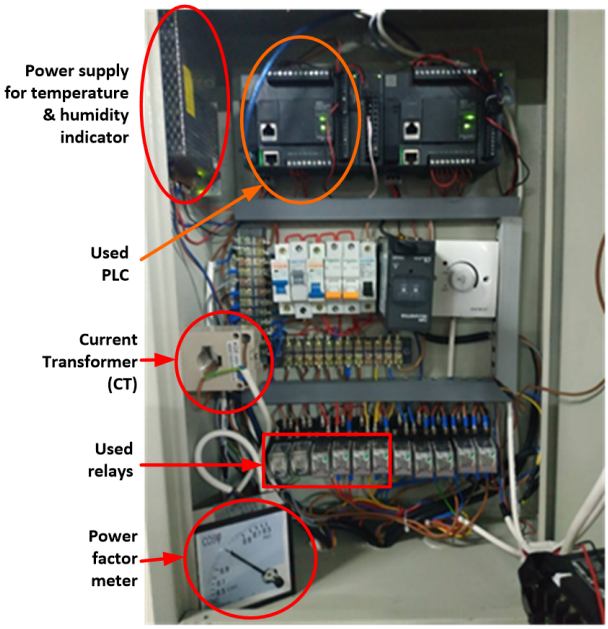

Fig. 4: *Realization of the control wiring in a panel box.*

to the controlled AC components, using six relays to control three compressors and three fan evaporators. The relays controlled the fan during high, medium, and low modes. Fig. 4 shows the realization of the control wiring system in the electrical panel box, with the circled parts indicating the main equipment used.

Table 2 presents the memory addresses of the ladder diagram, with the digital signals representing the PLC outputs and inputs. The input function was used for the on-off regulators and controlling components. The memory addresses were also used to store the commands in the system. The fan and compressor operated following the designed temperature and within a predetermined period. The fan operation follows the flowchart in Fig. 5.

The AC fans used three-speed modes when distributing cold air into the room: low, medium, and high. The fan speed operated following the temperature and switched automatically. The fan setting at low speed rotated at a room temperature below 23 ℃. When the room temperature rose to between 23 ℃ and 24 ℃, the fan automatically changed to medium speed, and when the room temperature rose to more than 24 ℃, the fan moved on to high or full speed. The three AC fans operated simultaneously at the same speed. The control circuit was installed using a 24 Vdc relay and the PLC provided the commands following the required modes. The fan rotations were 893.9 rpm, 801 rpm, and 702.2 rpm, at high, medium, and low speeds, respectively.

The room was conditioned with a temperature of 24 ℃ for human comfort. Therefore, it was necessary to create a temperature range for the three ACs to enable them to turn on and off. The first AC operated when the room temperature was above 26 ℃ and turned off at 23 ℃. Whereas the second AC operated at a temperature above 25 ℃ and turned off at 23 ℃. The third AC operated at a

Table 2: *Input and output addresses on the ladder diagram.*

Address	Input/Output/Memory	Digital/Analog	Function
%I0.0	Input	Digital	On
%I0.1	Input	Digital	Off
%Q0.0	Output	Digital	Fan High
%Q0.1	Output	Digital	Fan Medium
%Q0.2	Output	Digital	Fan Low
%Q0.3	Output	Digital	Compressor AC 1
%Q0.4	Output	Digital	Compressor AC 2
%Q0.5	Output	Digital	Compressor AC 3
%IW1.1	Input	Analog	Temperature
%IW1.2	Input	Analog	Humidity
%IW1.3	Input	Analog	Power
%M0	Memory	Digital	Autorun
%M1	Memory	Digital	System On
%M2	Memory	Digital	System Off
%M3	Memory	Digital	On AC 1 (temp.)
%M4	Memory	Digital	Off AC 1 (temp.)
%M5	Memory	Digital	On AC 2 (temp.)
%M6	Memory	Digital	Off AC 2 (temp.)
%M7	Memory	Digital	On AC 3 (temp.)
%M8	Memory	Digital	Off AC 3 (temp.)
%M9	Memory	Digital	AC 1 On
%M10	Memory	Digital	AC 1 Off
%M11	Memory	Digital	AC 2 On
%M12	Memory	Digital	AC 2 Off
%M13	Memory	Digital	AC 3 On
%M14	Memory	Digital	AC 3 Off

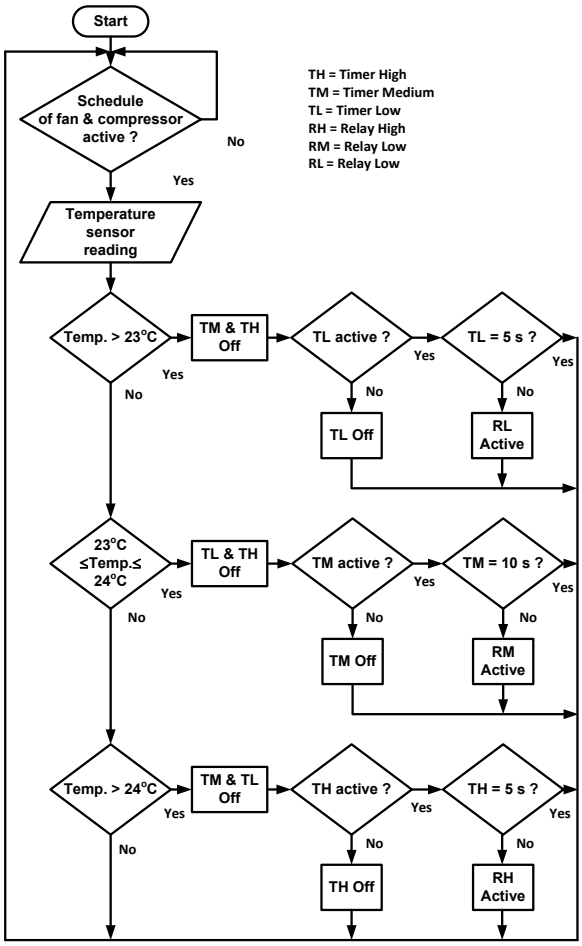

Fig. 5: *Flowchart showing the fan operational.*

temperature above 27 ℃ and turned off at 24 ℃. The first compressor operated at a temperature higher than 26 ℃ and turned off at 23 ℃. Whereas the second and third compressors operated at temperatures higher than 25 ℃ and 27 ℃, turning off at 23 ℃ and 24 ℃, respectively.

The next step involved integrating the PLC with SCADA to receive the data from the PLC transmitter. The temperature, humidity, and loading current data were sent via wireless and LAN communications, through a router. The SCADA recorded the power consumption, humidity, and temperature data every 30 minutes, which were subsequently saved in Word format. The AC testing was carried out in three stages. First, the air conditioners were operated conventionally, according to the manufacturer's system, without being regulated by the researcher. The air conditioner was set at a temperature of 18 ℃, to find a sufficiently close cool level to that in the manual mode, and ran from 09:00 to 18:00 on weekdays. The second test involved manual running the ACs, following the conditions of the room, according to the occupant's senses. When the occupant felt hot, the ACs were turned on, and off if the room felt cold. Thus, the AC fan modes ran accordingly. This test was also carried out from 09:00 to 18:00 on weekdays. For the third test, the ACs were run using PLC-based automatic running to achieve a comfortable room temperature. Based on the power used during every time interval, the energy consumed in a day was computed using numerical integration by applying the trapezoid composite rule (W_{trap}), and Simpson's composite rule (W_{simp}) [26] as well as ordinary (W_{ordi}) methods as presented in Eqs. (1), (2), and (3), respectively.

$$W_{trap} = \frac{h}{2}\left(P_0 + 2\sum_{k=1}^{n-1} P_k + P_n\right) \tag{1}$$

$$W_{simp} = \frac{h}{3}\left(P_0 + 4\sum_{k=1}^{n} P_{2k-1} + 2\sum_{k=1}^{n-1} P_{2k} + P_n\right) \tag{2}$$

$$W_{ordi} = \sum_{k=0}^{n-1} P_k \cdot h \tag{3}$$

where P_0, P_n, P_k, and h are the initiating power, ending power, k^{th} powers, and time step, respectively. The box plot method and outlier detection [27] were used to demonstrate the power trends for robust data analysis.

3. RESULTS AND DISCUSSION

3.1 Conventional AC System

Prior to testing the conventional system, it was assumed that the weekly load powers would be the

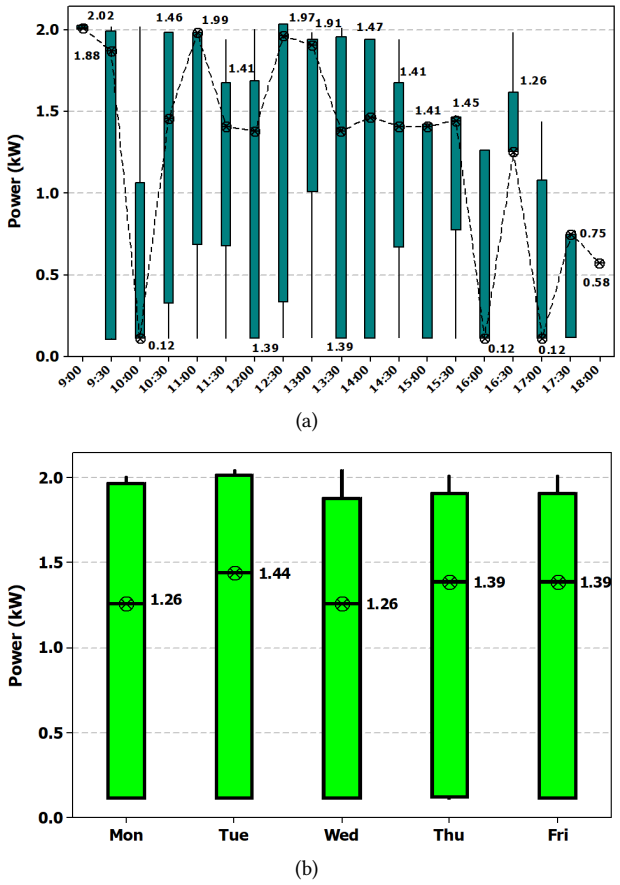

Fig. 6: *(a) Typical 30-minute and (b) daily conventional power consumption.*

same as other weeks. Fig. 6(a) shows the typical power consumption every 30 minutes during one weekday. In the morning, when the AC was turned on, the power absorbed jumped to adjust to the room conditions, temporarily decreasing afterward. However, the power consumption increased again with a rise in room temperature, caused by an increase in solar radiation and consequently the outside temperature. The power consumption reached the highest level during the day from around 12:30 to 14:00 when the room temperature reached its peak because the windows faced south. After midday, the power consumption decreased along with the room temperature, until the evening. Fig. 6(b) shows that the typical daily conventional power consumption remained fairly constant. However, the interquartile range (IQR) on Friday was the lowest compared to the other weekdays, probably due to a decrease in the occupant's working hours.

Table 3 presents the daily conventional energy consumption using three methods of computations: the trapezoidal composite rule, Simpson's composite rule, and ordinary. Generally, the highest power consumption took place on Monday and the lowest on Friday. This meant that on Friday, the occupant's activity was also the lowest. The energy consumption for a weekday was 48.5 kW·h, 49.7 kW·h, and 51.6 kW·h according to the trapezoidal composite rule (Trap.), Simpson's composite rule (Simp.), and ordinary (Ordi.) methods respectively. The ordinary computational method occupied the highest values due to it being the crudest.

Table 3: *Daily conventional energy consumption.*

Method	Mon	Tue	Wed	Thu	Fri
Trap.	10.2	10.0	9.8	9.7	8.8
Simp.	10.8	10.4	9.9	9.3	9.3
Ordi.	10.8	10.6	10.4	10.3	9.5

3.2 Manual AC System

The manual AC system was tested over a four-week period. Fig. 7(a) shows the typical level of manual power consumed in 30 minutes. Generally, in the mornings, power consumption increased until midday, decreasing down to zero at 18:00. Usually, the power consumption peaked between 12:00 until 14:00. Fig. 7(b) shows the typical daily power consumption. These values were relatively stable.

Table 4 shows the daily manual energy consumption using three computations: the trapezoidal composite rule, Simpson's composite rule, and ordinary methods. Generally, the ordinary computation yielded the highest values, since it was the crudest of the three. The energy consumption on Monday was usually the highest since, on these days, the occupant was very active.

3.3 Automatic AC System

Finally, the automatic PLC-based AC operation was tested. It operated automatically, following the designed control, to reach the set temperature for nine hours, starting at 09:00 and stopping at 18:00. The next timer operated for 15 hours, becoming the system downtime. The system returned to operation at 09:00 and continued to repeat every day, with the typical power consumption over 30 minutes, as shown in Fig. 8(a). Fig. 8(b) shows the typical daily power consumption of the automatic method. The degree of power consumed was similar, except for Monday, which was probably due to the previous day being a holiday so that the typical power was slightly higher than for the other weekdays.

Table 5 presents the comparative computations of automatic energy consumption. Generally, the ordinary method occupied the highest values for the energy consumed, since it was the crudest. While the lowest amount of energy was consumed on Wednesday.

Fig. 9(a) shows the comparative energy consumption during each weekday over a four-week period, using automatic, conventional, and manual methods. The automatic method resulted in the lowest energy consumption of the three, exhibiting a trapezoidal composite rule computation value of 150.8 kW·h. Whereas Simpson's composite rule and the ordinary computation consumed 152.6 kW·h and 154.4 kW·h, respectively. Fig. 9(b)

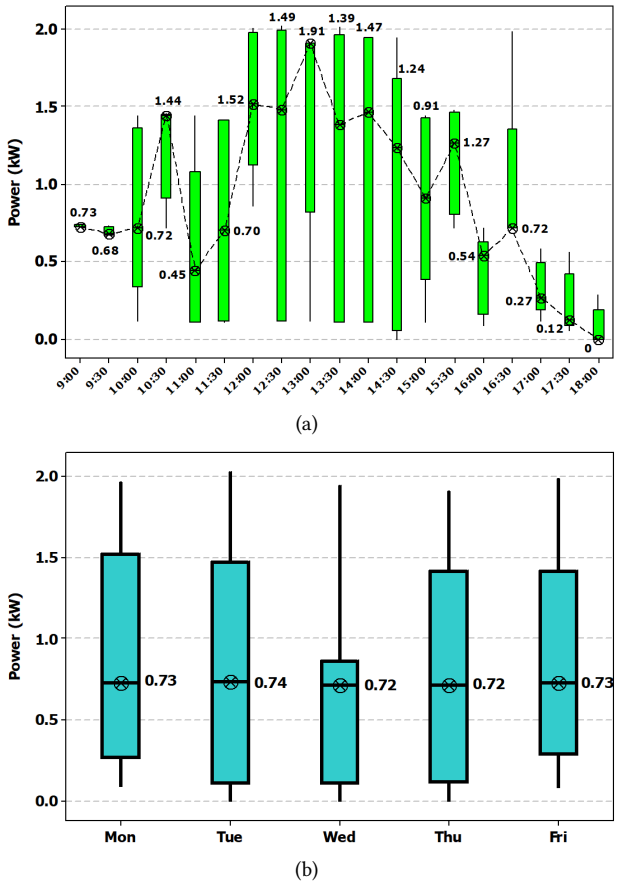

Fig. 7: *(a) Typical 30-minute room temperature and (b) daily manual power consumption.*

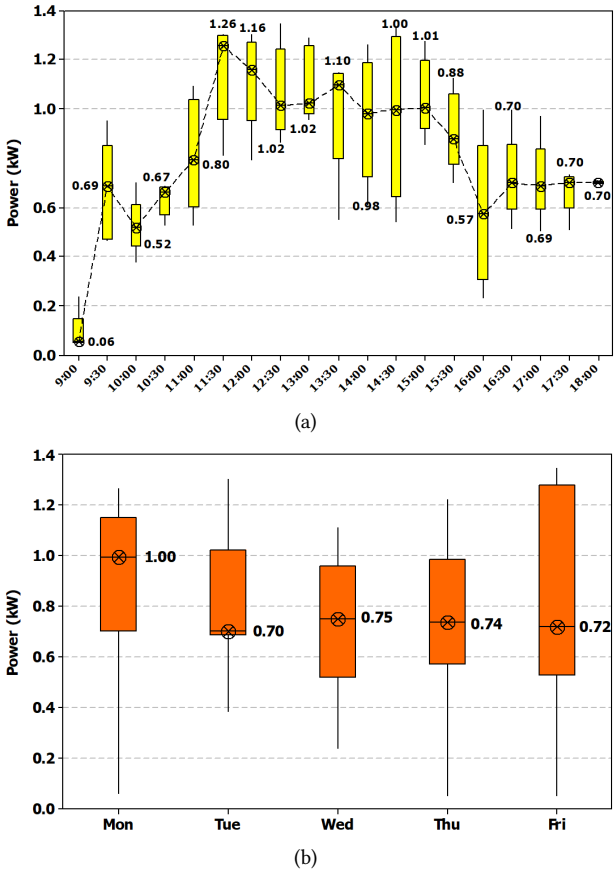

Fig. 8: *(a) Typical 30-minute room temperature and (b) daily automatic power consumption.*

Table 4: *Daily manual energy consumption.*

Week	Method	Mon	Tue	Wed	Thu	Fri	Total
1	Trap.	7.88	7.26	6.43	8.54	7.63	37.74
	Simp.	8.03	7.43	6.30	8.50	7.87	38.13
	Ordi.	8.07	7.45	6.80	8.73	7.84	38.89
2	Trap.	8.17	6.88	8.10	7.20	7.96	38.31
	Simp.	8.42	6.92	8.35	7.14	8.31	39.14
	Ordi.	8.36	7.07	8.29	7.38	8.15	39.25
3	Trap.	9.70	7.31	6.88	6.21	7.67	37.77
	Simp.	9.57	7.57	6.84	6.18	7.92	38.08
	Ordi.	9.89	7.50	7.07	6.40	7.86	38.72
4	Trap.	9.13	7.59	5.88	6.52	7.90	37.02
	Simp.	9.19	7.76	5.73	6.39	8.23	37.30
	Ordi.	9.32	7.78	6.07	6.40	8.09	37.66

Table 5: *Daily automatic energy consumption.*

Week	Method	Mon	Tue	Wed	Thu	Fri	Total
1	Trap.	8.26	8.03	6.97	8.07	8.11	39.44
	Simp.	8.08	7.64	6.09	8.23	7.83	37.87
	Ordi.	8.29	7.83	7.08	8.41	8.01	39.62
2	Trap.	8.57	8.47	7.20	7.03	9.34	40.61
	Simp.	8.92	8.31	7.25	6.99	9.00	40.47
	Ordi.	9.11	8.50	7.43	7.17	9.19	41.40
3	Trap.	9.27	8.35	6.23	7.49	9.02	40.36
	Simp.	9.61	8.19	6.16	7.30	8.53	39.79
	Ordi.	9.82	8.38	6.34	7.49	8.86	40.89
4	Trap.	9.31	8.19	6.97	6.80	8.85	40.12
	Simp.	9.67	7.95	6.90	6.64	8.27	39.43
	Ordi.	9.88	8.14	7.08	6.82	8.60	40.52

shows the percentage of energy savings resulting from the automatic-to-manual and automatic-to-conventional methods.

These energy savings resulted from the ACs following the temperature level for optimal comfort. The ACs consumed more electrical energy with the conventional method for several reasons. For instance, the temperature on the AC remote was set at 18 ℃, which meant that for optimal operation, the ACs had to turn on continuously due to the fan setting of the high state evaporator. It was difficult to reach the desired temperature because when the fan was spinning at the maximum (high) level, it operated continuously to distribute cold air from the system, causing the temperature in the evaporator to rise again. In the automatic system, the fan operated automatically, following the temperature. When it was cold, the fan operated at the minimum (low) level, increasing to maximum when the temperature was high. The conventional AC operated according to the temperature reading provided by the thermistor in the evaporator. The temperature represented the target of

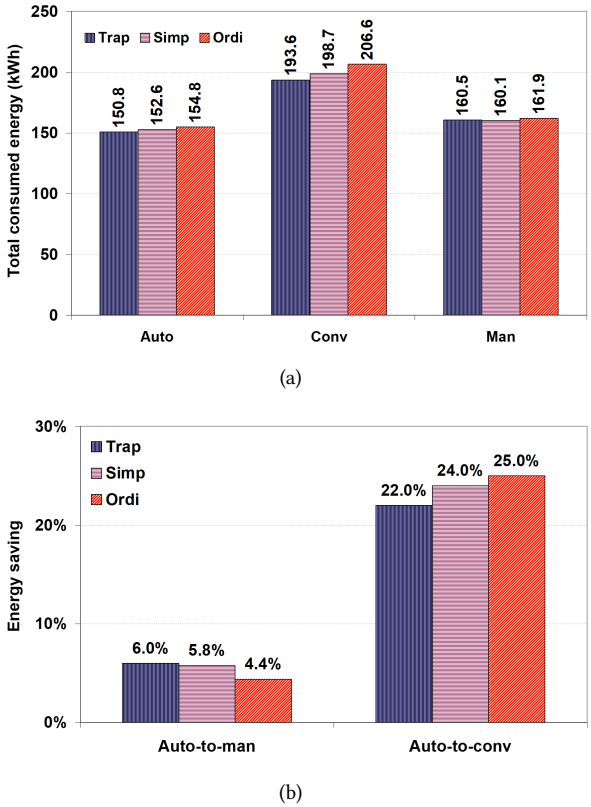

Fig. 9: *(a) Energy consumption and (b) energy savings.*

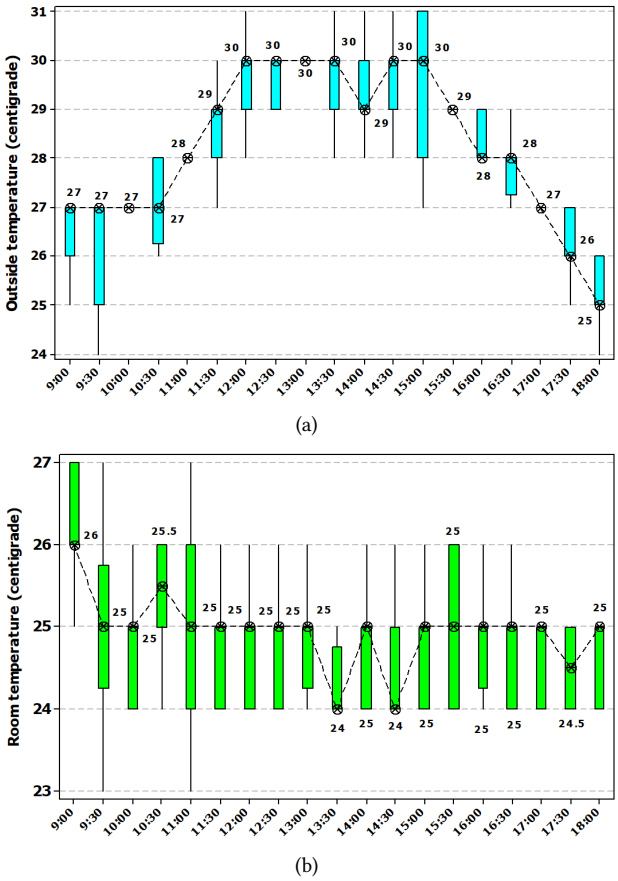

Fig. 10: *Typical 30-minute room temperature (a) outside and (b) maintained.*

the thermostat in the system. Thus, there was often a difference in the room and remote temperatures.

The effect of installing temperature sensors on the conventional and PLC-based automatic operations was highly influential in achieving energy savings because these methods used the sensor to read the room temperature, following the room conditions and comfort level. The automatic method, compared to the manual method, provided energy savings of 6% (composite trapezoidal rule), 5.8% (composite Simpson's rule), and 4.4% (ordinary rule). The difference between both systems was not very significant because the manual system operated using the level of human comfort so that it was almost the same as the automatic system. Nevertheless, the manual system did not always pay attention to the level of comfort, frequently forgetting to operate the AC efficiently, resulting in greater energy consumption than the automatic system. Whereas the automatic-to-conventional method provided energy savings of 22.0%, 24.0%, and 25.0% for the trapezoidal composite rule, Simpson's composite rule, and ordinary, respectively. These comparisons demonstrate that the automatic system was the most efficient way to regulate the room to provide a comfortable temperature.

The first savings were within the expected range and the second savings higher than [5], at 11.31%, 5.10%, and 7.80%. Both savings were lower than 30–40% [6], and range from 10–15% [7], 5.6% [11], 14% [17], 1.15–39.79% [22], and 20% [24]. Thus, the automatic operation of ACs in this study yielded significant energy savings.

3.4 Power Influence on Temperature and Humidity

Fig. 10(a) shows the typical daily outside temperature. In the morning, the temperature rose, reaching the maximum value from 12:00 to 15:00. Fig. 10(b) shows the typical room temperature when automatically conditioned. The temperature was typically stable at around 25 ℃. Thus, the automatic method could effectively maintain the room temperature.

Fig. 11(a) shows the normalized temperature versus the AC power consumption. If the outside temperature remained constant, it would stay the same as it was at the start of the day (09:00). As the power consumption increased, the normalized temperature decreased significantly, at an average rate of −5.27 ℃/kW. Fig. 11(b) shows the difference in the scatter and regression plots between the outside-to-room temperature and power consumption. Generally, the temperature difference increased along with the power consumption, at an average rate of 2.99 ℃/kW. The median values of the box plots also indicated an increasing trend, as shown in Fig. 11(c).

Fig. 12(a) shows the typical difference between the outside and room temperatures. At the start of the day (09:00), no difference in temperature was assumed. The

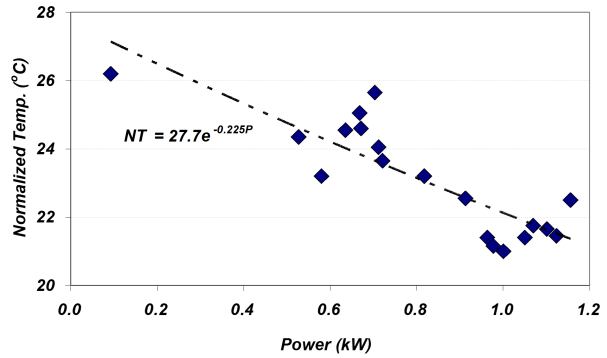

(a)

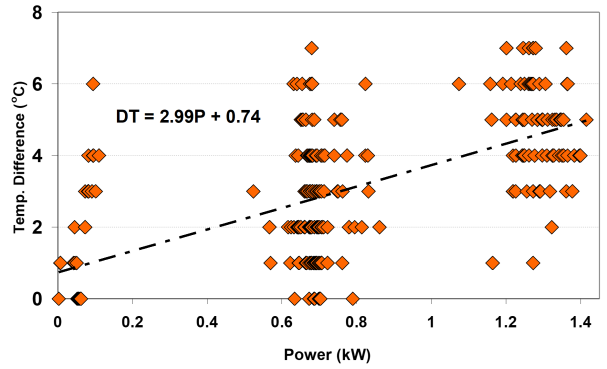

(b)

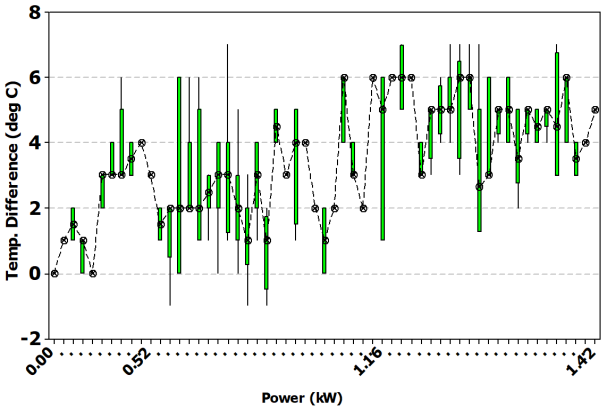

(c)

Fig. 11: *(a) Normalized temperature, (b) scatter-regression plots, and (c) typical difference between temperature and power consumption.*

temperature difference increased and reached a peak at around 13:30, subsequently decreasing until 18:00, when the typical temperature difference was no more than 1 ℃. Fig. 12(b) shows the average scatter and regression plots of the room temperature compared to the AC power consumption using the automatic method. As the power consumption increased, the temperature tended to be fairly constant at around 25 ℃. The increasing power consumption was caused by the room temperature being maintained as the outside temperature rose. The three scatter plots were caused by one, two, and three AC operations, respectively.

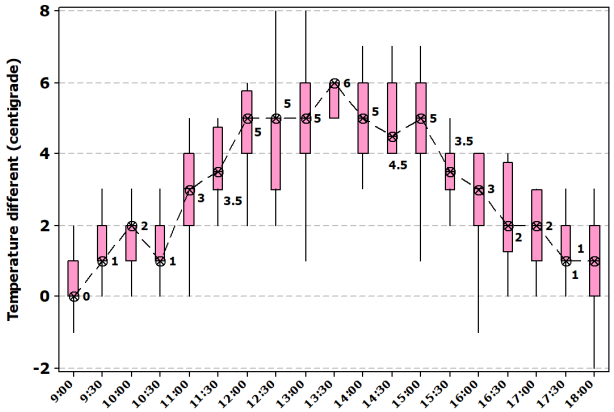

(a)

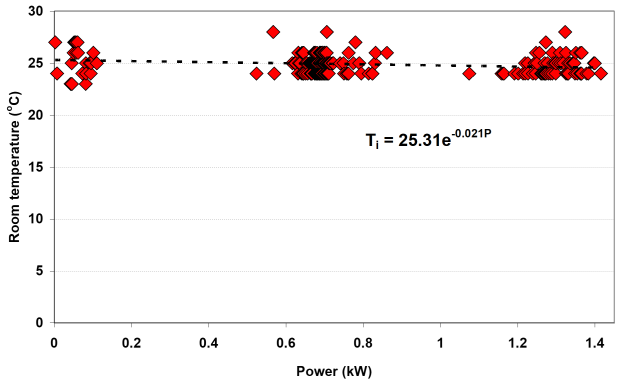

(b)

Fig. 12: *(a) Typical 30-minute temperature difference and (b) room temperature versus power.*

Fig. 13(a) shows the average scatter and regression plots of the room humidity compared to power consumption using the automatic AC. The results show that as the power consumption increased, the room humidity decreased considerably, at a rate of −10.03 %RH/kW. This trend was comparable to the box plot median values, as shown in Fig. 13(b). Based on the boxplot median values, the average reduction in relative humidity caused by increasing power was −4.23 %RH/kW.

The decreasing relative humidity (RH) resulting from the increase in power consumption was due to the water content in the air being blown away by the AC blower, despite a decrease in air temperature. Thus, provided the temperature remained constant in the air-conditioned room, and even fell, the humidity also dropped. This is rather different to atmospheric conditions where humidity decreases as the temperature increases [28].

4. CONCLUSION

The control process of the PLC-based automatic system for AC energy-saving proved to be successful. The PLC was combined with a 4–20 mA analog module for signal transmission of the temperature, humidity, and loading current. The energy savings between the PLC-based automatic and conventional systems were 22.0%,

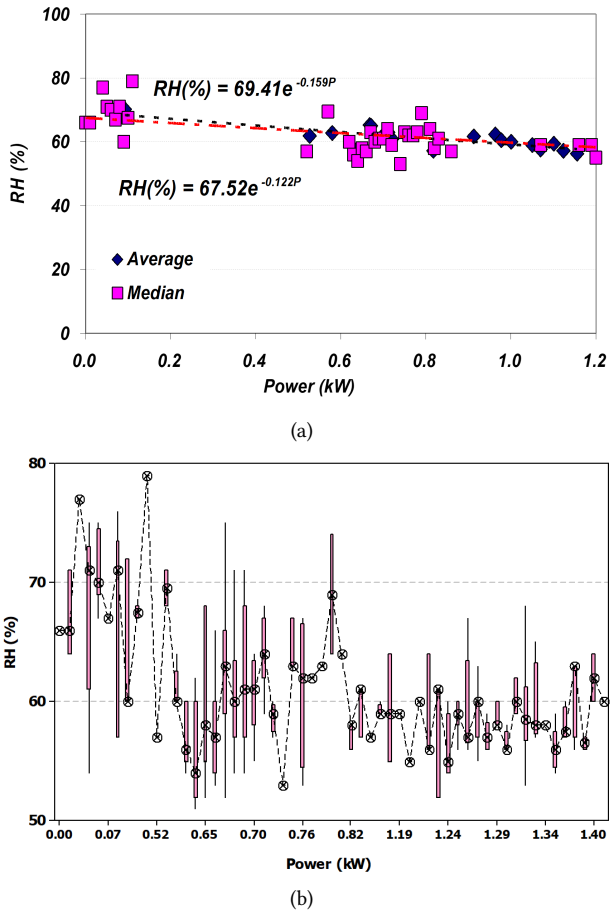

Fig. 13: (a) Average scatter and regression and (b) box plots showing median room humidity versus power.

24.0%, and 25.0%, and between the PLC-based automatic and manual systems 6.0%, 5.8%, and 4.4%, respectively using the composite trapezoidal rule, composite Simpson's rule, and ordinary methods. The normalized temperature decreased as the power consumption increased, at a rate of −5.27 ℃/kW. Whereas, the rate of the decreasing RH was −10.03 %RH/kW and −4.23 %RH/kW, based on the average and median values, respectively.

ACKNOWLEDGMENT

This research is supported in part by the Directorate of Research and Community Service, Directorate General of Research Strengthening and Development, Ministry of Research, Technology and Higher Education, Indonesia, under Grant No. 245/B.05/LPPM-Itenas/II/2018.

REFERENCES

[1] J. Tomczyk, E. Silberstein, B. Whitman, and B. Johnson, *Refrigeration and Air Conditioning Technology*, 8th ed. Boston, MA, USA: Cengage Learning, 2016.

[2] G. F. Hundy, A. R. Trott, and T. C. Welch, *Refrigeration, Air Conditioning, and Heat Pumps*, 5th ed. Oxford, UK: Butterworth-Heinemann, 2016.

[3] N. E. Wijeysundera, *Principles Of Heating, Ventilation And Air Conditioning with Worked Examples*. Singapore: World Scientific Publishing, 2016.

[4] G. Lippsmeier, *Tropenbau: Building in the Tropics*. Munich, Germany: Callway Verlag, 1980.

[5] W. Song, J. Yang, Y. Ji, and C. Zhang, "Experimental study on characteristics of a dual temperature control valve in the chilled water system of an air-conditioning unit," *Energy and Buildings*, vol. 202, Nov. 2019, Art. no. 109369.

[6] G. Escrivá-Escrivá, "Basic actions to improve energy efficiency in commercial buildings in operation," *Energy and Buildings*, vol. 43, no. 11, pp. 3106–3111, Nov. 2011.

[7] M. Batić, N. Tomašević, G. Beccuti, T. Demiray, and S. Vraneš, "Combined energy hub optimisation and demand side management for buildings," *Energy and Buildings*, vol. 127, pp. 229–241, Sep. 2016.

[8] M. Verde, K. Harby, R. de Boer, and J. M. Corberán, "Performance evaluation of a waste-heat driven adsorption system for automotive air-conditioning: Part I – modeling and experimental validation," *Energy*, vol. 116, pp. 526–538, Dec. 2016.

[9] X. Li, T. Zhao, P. Fan, and J. Zhang, "Rule-based fuzzy control method for static pressure reset using improved mamdani model in VAV systems," *Journal of Building Engineering*, vol. 22, pp. 192–199, Mar. 2019.

[10] X. Li, T. Zhao, J. Zhang, and T. Chen, "Development of network control platform for energy saving of fan coil units," *Journal of Building Engineering*, vol. 12, pp. 155–160, Jul. 2017.

[11] Z. Wu, Q.-S. Jia, and X. Guan, "Optimal control of multiroom HVAC system: An event-based approach," *IEEE Transactions on Control Systems Technology*, vol. 24, no. 2, pp. 662–669, Mar. 2016.

[12] N. Radhakrishnan, S. Srinivasan, R. Su, and K. Poolla, "Learning-based hierarchical distributed HVAC scheduling with operational constraints," *IEEE Transactions on Control Systems Technology*, vol. 26, no. 5, pp. 1892–1900, Sep. 2018.

[13] H.-C. Jo, S. Kim, and S.-K. Joo, "Smart heating and air conditioning scheduling method incorporating customer convenience for home energy management system," *IEEE Transactions on Consumer Electronics*, vol. 59, no. 2, pp. 316–322, May 2013.

[14] W. Bolton, *Programmable Logic Controllers*, 6th ed. Oxford, UK: Newnes, 2015.

[15] C. Chiou, C. Chiou, C. Chu, and S. Lin, "The application of fuzzy control on energy saving for multi-unit room air-conditioners," *Applied Thermal Engineering*, vol. 29, no. 2-3, pp. 310–316, Feb. 2009.

[16] S. Soyguder and H. Alli, "Predicting of fan speed for energy saving in HVAC system based on adaptive network based fuzzy inference system," *Expert Systems with Applications*, vol. 36, no. 4, pp. 8631–8638, May 2009.

[17] Q. P. Ha and V. Vakiloroaya, "Modeling and optimal control of an energy-efficient hybrid solar air condi-

tioning system," *Automation in Construction*, vol. 49, Part B, pp. 262–270, Jan. 2015.
[18] P. Zhang, D. Zhou, W. Shi, X. Li, and B. Wang, "Dynamic performance of self-operated three-way valve used in a hybrid air conditioner," *Applied Thermal Engineering*, vol. 65, no. 1–2, pp. 384–393, Apr. 2014.
[19] Z. Meng, H. Zhang, M. Lei, Y. Qin, and J. Qiu, "Performance of low GWP r1234yf/r134a mixture as a replacement for r134a in automotive air conditioning systems," *International Journal of Heat and Mass Transfer*, vol. 116, pp. 362–370, Jan. 2018.
[20] Q. P. Ha and V. Vakiloroaya, "A novel solar-assisted air-conditioner system for energy savings with performance enhancement," *Procedia Engineering*, vol. 49, pp. 116–123, 2012.
[21] D. La, Y. Dai, Y. Li, T. Ge, and R. Wang, "Study on a novel thermally driven air conditioning system with desiccant dehumidification and regenerative evaporative cooling," *Building and Environment*, vol. 45, no. 11, pp. 2473–2484, Nov. 2010.
[22] I. Sarbu and M. Adam, "Experimental and numerical investigations of the energy efficiency of conventional air conditioning systems in cooling mode and comfort assurance in office buildings," *Energy and Buildings*, vol. 85, pp. 45–58, Dec. 2014.
[23] S. Somasundaram, S. R. Thangavelu, and A. Chong, "Improving building efficiency using low-e coating based retrofit double glazing with solar films," *Applied Thermal Engineering*, vol. 171, May 2020, Art. no. 115064.
[24] A. Spagnuolo, A. Petraglia, C. Vetromile, R. Formosi, and C. Lubritto, "Monitoring and optimization of energy consumption of base transceiver stations," *Energy*, vol. 81, pp. 286–293, Mar. 2015.
[25] X. Su, S. Tian, X. Shao, and X. Zhang, "Experimental and numerical study on low temperature regeneration desiccant wheel: Parameter analysis with a comprehensive energy index," *International Journal of Refrigeration*, vol. 120, pp. 237–247, Dec. 2020.
[26] M. K. Jain, S. R. K. Iyengar, and R. K. Jain, *Numerical Methods (Problems and Solutions)*, 2nd ed. Delhi, India: New Age International, 2007.
[27] C. Zhao and J. Yang, "A robust skewed boxplot for detecting outliers in rainfall observations in real-time flood forecasting," *Advances in Meteorology*, vol. 2019, 2019, Art. no. 1795673.
[28] E. Hosseinian, P.-O. Theillet, and O. Pierron, "Temperature and humidity effects on the quality factor of a silicon lateral rotary micro-resonator in atmospheric air," *Sensors and Actuators A: Physical*, vol. 189, pp. 380–389, Jan. 2013.

Waluyo received master's and doctoral degrees in high voltage engineering from the Institut Teknologi Bandung, Bandung, Indonesia, in 2002 and 2010, respectively. He is currently an Associate Professor with the Department of Electrical Engineering, Institut Teknologi Nasional Bandung, Indonesia. His research interests include high voltage engineering and technology, power transmission, smart grid, and automation systems.

Andre Widura received a master's degree in biomedical engineering from the Institut Teknologi Bandung (ITB), Indonesia, in 2010. He is currently an academic staff with the Department of Electrical Engineering, Institut Teknologi Nasional Bandung, Indonesia. His research interests include biomedical engineering, solar cell, and battery.

Wahyu Agung Purbandoko received a bachelor's degree in electrical engineering from the Institut Teknologi Nasional Bandung, Indonesia, in 2019. He is currently a staff with a private company. His research interests include automation systems and heating, ventilating, and air conditioning.